

1 **Comprehensive antibody profiling of mRNA vaccination in children**

2 **Authors:** Yannic C Bartsch, PhD ¹; Kerri J St Denis¹; Paulina Kaplonek, PhD ; Jaewon Kang¹;
3 Evan C. Lam¹; Madeleine D Burns²; Eva J Farkas²; Jameson P Davis²; Brittany P Boribong, PhD
4 ²; Andrea G Edlow, MD³; Alessio Fasano, MD²; Wayne Shreffler, MD PhD⁴; Dace Zavadska, MD
5 PhD⁵; Marina Johnson, PhD⁶; David Goldblatt, PhD⁶; Alejandro B Balazs, PhD¹; Lael M Yonker,
6 MD^{2#}; Galit Alter, PhD ^{1#}

7 **Affiliations:**

8 ¹ Ragon Institute of MGH, MIT, and Harvard, Cambridge, MA, USA

9 ² Massachusetts General Hospital Department of Pediatrics, Mucosal Immunology and Biology
10 Research Center, Boston, MA, USA

11 ³ Massachusetts General Hospital Department of Obstetrics and Gynecology, Division of
12 Maternal-Fetal Medicine, Vincent Center for Reproductive Biology, Boston, MA, USA

13 ⁴ Massachusetts General Hospital Food Allergy Center, Division of Pediatric Allergy and
14 Immunology, Boston, MA, USA

15 ⁵ Children's Clinical University Hospital, Riga, Latvia

16 ⁶ Great Ormond Street Institute of Child Health Biomedical Research Centre, University College
17 London, London, UK

18

19 *correspondence: LYONKER@mgh.harvard.edu and GALTER@mgh.harvard.edu

20

21 **Abstract:** While children have been largely spared from COVID-19 disease, the emergence of
22 viral variants of concern (VOC) with increased transmissibility, combined with fluctuating mask
23 mandates and school re-openings have led to increased infections and disease among children.
24 Thus, there is an urgent need to roll out COVID-19 vaccines to children of all ages. However,
25 whether children respond equivalently to adults to mRNA vaccines and whether dosing will elicit
26 optimal immunity remains unclear. Given the recent announcement of incomplete immunity
27 induced by the pediatric dose of the BNT162b2 vaccine in young children, here we aimed to deeply
28 profile and compare the vaccine-induced humoral immune response in 6-11 year old children
29 receiving the pediatric (50 μ g) or adult (100 μ g) dose of the mRNA-1273 vaccine compared to
30 adults and naturally infected children or children that experienced multi inflammatory syndrome
31 in children (MIS-C) for the first time. Children elicited an IgG dominant vaccine induced immune
32 response, surpassing adults at a matched 100 μ g dose, but more variable immunity at a 50 μ g dose.
33 Irrespective of titer, children generated antibodies with enhanced Fc-receptor binding capacity.
34 Moreover, like adults, children generated cross-VOC humoral immunity, marked by a decline of
35 omicron receptor binding domain-binding, but robustly preserved omicron Spike-receptor binding,
36 with robustly preserved Fc-receptor binding capabilities, in a dose dependent manner. These data
37 indicate that while both 50 μ g and 100 μ g of mRNA vaccination in children elicits robust cross-
38 VOC antibody responses, 100 μ g of mRNA in children results in highly preserved omicron-specific
39 functional humoral immunity.

40 **One-Sentence Summary:** mRNA vaccination elicits robust humoral immune responses to SARS-
41 CoV-2 in children 6-11 years of age.

42 **Introduction**

43 The burden of respiratory infections is often higher in young children with a developing untrained
44 immune system(1). However, lower rates of disease were noted early in the COVID-19 pandemic
45 among children, who largely experienced asymptomatic or pauci-symptomatic SARS-CoV-2
46 infections(2). However, with the rise of highly infectious variants of concern (VOCs), like the
47 novel omicron VOC, increasing infection rates and hospitalizations have been observed globally(3,
48 4). Linked to the unpredictable incidence of multisystem inflammatory syndrome in children
49 (MIS-C) and the clear contribution children make to population level spread, the need for vaccines
50 for children is evident (5, 6). However, whether newly emerging COVID-19 vaccine platforms,
51 approved for teenager/adult use, elicit immunity in children is not well understood.

52 Epidemiologic data clearly highlight vulnerabilities in the pediatric immune system, with
53 increased rates of respiratory, enteric, and parasitic infections disproportionately causing disease
54 in children in the first decade of life(7, 8). In fact, vaccine-induced immune responses often differ
55 across children and adults(9). However, whether these vulnerabilities to infection and poor
56 response to protein-based vaccination will translate to newer vaccine platforms, like mRNA
57 vaccine platforms, remains unclear. Moreover, emerging data suggests that dosing may not be
58 straight forward for mRNA vaccines (10, 11), due to reduced immunogenicity in young children,
59 requiring deeper immunologic insights to guide rational pediatric vaccine design.

60 To begin to define the humoral mRNA vaccine responses in children, we comprehensively profiled
61 vaccine-induced immune responses in children (6-11 years) who received the pediatric (50µg) or
62 adult (100µg) dose of the mRNA-1273 vaccine regimen, respectively. We observed 100% vaccine
63 response rates prior to the second vaccine dose in children that received the 100µg vaccine dose.
64 While immune profiles in the low (50µg) dose were more similar to adults (who received the adults

65 recommended 100 μ g dose), children receiving the adult (100 μ g) dose generated disproportionately
66 higher IgG biased vaccine responses following the second vaccine dose, with enhanced Fc-effector
67 profiles. Moreover, both pediatric and adult doses elicited broad cross-variant isotype and Fc-
68 receptor binding antibodies, however, while all groups experienced a significant loss of omicron-
69 receptor binding domain (RBD) reactivity, omicron Spike-specific immunity was largely
70 preserved and 100 μ g immunized children exhibited the highest cross-reactivity. Collectively, these
71 data point to robust, but dose dependent, functional humoral pediatric immune signatures induced
72 in children following mRNA-1273 vaccination.

73 **Results**

74 In the wake of fluctuating mask mandates, school re-openings, and the rapid spread of the highly
75 infectious SARS-CoV-2 delta and omicron variants, a surge of SARS-CoV-2 infections in children
76 has been observed (5). Increasing numbers of children with severe COVID-19 or life-threatening
77 Multisystem Inflammatory Syndrome in Children (MIS-C), plus our evolving appreciation of
78 children in the spread of the pandemic, there is an urgent need to roll out vaccines across all ages.
79 With the rapid roll out of mRNA vaccines, it remains unclear whether children will generate
80 sufficiently robust immunity following mRNA vaccination. Here we deeply characterized the
81 immune response induced by the Moderna mRNA-1273 vaccine in children that received an adult
82 dose (100 μ g) of mRNA-1273 (n=12; median age= 9 years range: 7 – 11 years; 42% female),
83 matching the recommendations for adults, or a pediatric (50 μ g) dose of mRNA-1273 (n=12;
84 median age= 8 years range: 5 – 11 years; 50% female) at days 0 and 28, respectively. Plasma
85 samples were collected before vaccination (V0), approximately four weeks after prime (V1) and
86 four weeks after second (V2) immunization.

87 *mRNA vaccines induce robust SARS-CoV-2 spike binding and neutralizing titers in children*

88 To begin to investigate the vaccine-induced humoral response, we profiled SARS-CoV-2 Spike
89 (S) specific antibody titers. At V1, we observed seroconversion (marked by an increase in Spike
90 specific IgM, IgA1 or IgG1 binding compared to V0) in 100 % of children receiving the 50 μ g
91 (n=9/9) or 100 μ g (n=12/12) dose of mRNA-1273. Both S-specific IgA1 and IgG1 increased with
92 the second dose, while S-specific IgM responses declined slightly, marking efficient class
93 switching. After the second dose we observed significantly elevated S-specific IgA1 levels in
94 adults compared to children (p-value: <0.001) (**Figure 1A**). In contrast, children in the 100 μ g dose
95 group elicited higher IgG1 titers after the first and second dose of the vaccine compared to children
96 in the 50 μ g dose group (p-value: 0.004), as well as compared to vaccinated adults (p-value: 0.03).
97 Likewise, we observed a trend towards higher neutralizing antibody titers in the pediatric 100 μ g
98 dose group followed by adults and 50 μ g vaccinated children (**Figure 1B**). Univariate comparison
99 of V2 levels of the 100 μ g adults to 100 μ g and 50 μ g children highlighted isotype selection
100 differences across children and adults, but minimal overall differences in antibody binding titers
101 and neutralization across the 50 and 100 μ g doses in children (**Figure 1C**). Furthermore, vaccine-
102 induced binding and neutralization titers in the 100 μ g pediatric dose group were higher compared
103 to levels observed in naturally exposed convalescent children or MIS-C. Importantly, while these
104 differences may be related to exposure to different variants, we observed superior vaccine induced
105 binding and neutralization to all variants, highlighting the critical importance of SARS-CoV-2
106 vaccination in promoting broader VOC immunity in children compared to infection
107 (**Supplemental Figure 1 and 2**). Taken together, these data show that mRNA vaccination can
108 elicit strong but dose-dependent anti-SARS-CoV-2 binding and neutralizing titers in children
109 superior to natural infection that are accompanied by some age-dependent shifts in isotype-
110 antibody profiles.

111 *mRNA vaccination induces highly potent Spike-specific Fc effector functions in children*

112 In addition to binding and neutralization, protection against severe adult COVID-19 has been
113 linked to the ability of antibodies to leverage additional antiviral functions via Fc-receptors to fight
114 infection, referred to as antibody effector functions(12-14). Specifically, opsonophagocytic
115 pathogen clearance is key to protection against several bacterial pathogens and cytotoxic antibody
116 functions have been linked to protection against viruses(15, 16). Thus, we profiled the relative
117 ability of vaccine-induced immune responses to bind to human Fc-receptors (Fc γ R2a, Fc γ R2b,
118 Fc γ R3a, Fc γ R3b, and Fc α R) as well as their ability to elicit antibody-dependent complement
119 deposition (ADCD), antibody dependent neutrophil phagocytosis (ADNP), antibody dependent
120 monocyte phagocytosis (ADCP), or activation antibody dependent NK cell activation (ADNKA).
121 Children in both dose groups elicited Spike (S)-specific IgG antibodies that bound robustly to all
122 Fc-receptors following the first dose, markedly greater than responses observed in vaccinated
123 adults and in natural COVID-19 infection or MIS-C (**Figure 2A**). Moreover, these responses
124 expanded further after the second immunization with significantly elevated antibody-Fc-receptor
125 binding in the 100 μ g pediatric dose group compared to the 50 μ g dose, with significant higher
126 Fc γ R3a and slightly higher Fc γ R2a, Fc γ R2b and Fc γ R3b binding compared to the 100 μ g adult
127 group (**Figure 2B**). Interestingly, this increased Fc-receptor binding was not directly related to
128 overall changes in Spike-specific IgG subclass selection (**Supplemental Figure 1**), pointing to
129 alternate mechanisms for augmented humoral immune function in children, potentially linked to
130 pediatric selection of more potent Fc-glycosylation profiles(17). In contrast, compared to adults,
131 children induced lower levels of IgA antibodies that exhibited, as expected, lower interactions with
132 the IgA-Fc-receptor, Fc α R, compared to adults (**Figure 2B and Supplemental Figure 2**)(18, 19).

133 To next determine whether these distinct pediatric Fc γ -receptor binding profiles translated to more
134 functional Spike-specific humoral immune responses, we examined vaccine-induced Fc-effector
135 functions (**Figure 2C**). Interestingly, low levels of ADCD, ADNP and ADCP were observed after
136 primary immunization, but were notably augmented by the second immunization across the
137 groups, resulting in significantly increased ADCD and ADNP in the 100 μ g vaccinated children
138 compared to adults or the 50 μ g pediatric dose (**Figure 2C**). In contrast, NK cell functions (as
139 measured by MIP-1b expression) were induced to equal levels across all groups. Overall, high
140 dose mRNA-1273 induced higher levels of ADCD, ADNP and ADCP recruiting antibodies in
141 children compared to adults following the 100 μ g vaccine regimen (**Figure 2D**). These data point
142 to enhanced functional antibody responsiveness in children at a matched 100 μ g dose compared to
143 adults, and a solid functional response at the optimized 50 μ g dose endowing children with a robust
144 capacity to recruit immune function at half the adult dose, all higher than levels observed following
145 natural infection or MIS-C.

146 *Selective expansion of opsonophagocytic antibodies with mRNA vaccination in children*

147 To gain a more granular sense of the differences in immune responses across children and adults
148 at the same matched dose or across children receiving the 50 and 100 μ g doses, we next utilized a
149 machine learning approach to probe the humoral immune features that differed most across these
150 groups. As few as six of the overall features analyzed across all plasma samples, were sufficient
151 to completely resolve vaccine induced immune responses induced by the 100 μ g dose across
152 children and adults (**Figure 3A+B**). Specifically, vaccine-induced S-specific IgG1, Fc γ R3a
153 binding, ADNP and ADCD were all enriched selectively in children, whereas Spike-specific IgM
154 and IgA1 titers were enriched in adults (**Figure 3A**), highlighting distinct isotype selection in
155 adults, and the generation of more functional antibodies in children. Conversely, comparison of

156 50 and 100 μ g doses in children was achieved using only two of all antibody features analyzed
157 for each plasma. These features Spike-specific ADNP and IgG4 levels, both of which were
158 enriched in the immune profiles in children that received the 100 μ g dose of the vaccine (**Figure**
159 **3C+D**). Additionally, in contrast to natural infection, vaccination induced higher titers and
160 functions to SARS-CoV-2 when comparing vaccinated children to those that were previously
161 infected (**Figure 2 and Supplemental Figure 3**). Collectively, these data point to slight shifts in
162 isotype selection between adults and children, but the potential for children to raise more
163 functional antibodies, that match those of adults at a half-dose.

164 *mRNA vaccination in children raises robust responses against SARS-CoV-2 variants of concern*

165 Real-world efficacy suggests that mRNA vaccines confer robust protection against severe
166 disease/death against the original (wildtype; wt) SARS-CoV-2 strain (Wuhan), at levels greater
167 than 90% (20). This level of efficacy appears to be sustained against evolving variants of concern
168 (VOCs), including the alpha and delta variants, although lower levels of protection have been
169 observed against the beta variant (21, 22). While previous VOCs were marked by single or few
170 amino acid substitutions, the novel omicron variant has 29 mutations in the Spike protein, resulting
171 in enhanced transmissibility, and a concomitant loss of neutralizing titers (23, 24). Yet, despite the
172 striking increase in omicron transmissibility, a similar increase in severe disease and death has not
173 been observed, suggesting that alternate vaccine induced immune responses may continue to afford
174 protection against severe disease and death. To explore whether mRNA vaccination in children
175 results in the generation of vaccines with differential VOC recognition capabilities (25). We
176 observed a progressive loss of IgM, IgA, and IgG binding to VOC RBDs across both pediatric
177 groups and adults, with more variable cross-VOC IgG responses among 50 μ g immunized children,
178 but a consistent and significant loss of binding to the omicron RBD across all 3 groups (Figure

179 4A). Conversely, Spike-specific responses were more resilient across most VOCs, across the 3
180 groups, except for omicron-Spike-specific responses that were significantly lower across IgM and
181 IgA response across the groups (Figure 4B). Yet, IgG responses showed 3 different patterns: 1)
182 50 μ g immunized children experienced heterogeneous responses across VOCs, marked by some of
183 the lowest omicron-responses, 2) adults exhibited more stable Spike VOC-IgG binding levels, but
184 experienced a significant reduction in omicron-Spike reactivity, and 3) 100 μ g immunized children
185 exhibited negligible reduction in Spike-specific recognition across VOCs, including to the omicron
186 Spike. Furthermore, Fc-receptor binding capability was largely preserved across RBD VOCs,
187 except for omicron RBD-binding which was significantly lower across all 3 groups (Figure 4C).
188 However, Spike-VOC binding differed across the 3 groups. While wildtype, alpha, beta, and delta
189 VOC Fc-receptor binding profiles were highly preserved across all 3 groups, omicron-Spike Fc-
190 receptor binding was most significantly lost in 50 μ g immunized children (Figure 4D). Adults
191 exhibited an intermediate loss of omicron-Spike Fc-receptor binding, with a more pronounced
192 preservation of the opsonophagocytic Fc γ R2a and cytotoxic Fc γ R3a binding. Conversely, 100 μ g
193 immunized children exhibited a negligible loss of Fc-receptor binding to the omicron Spike,
194 pointing to the generation of highly resilient antibodies in children at the adult dose that continue
195 to bind to the omicron Spike despite the significant loss of RBD binding. Whether children
196 generate broader or more flexible humoral immune response at the 100 μ g dose, enabling them to
197 preserve immunity to VOCs remains unclear, but the data point to dose and age dependent effects
198 of antibody-mediated cross-VOC recognition. Whether differences in neutralization and Fc-
199 function lead to differences in disease-breakthrough across the ages remains unclear but provides
200 some additional immunological insights that may continue to explain the epidemiologic
201 differences in disease severity globally in the setting of emerging VOCs.

202

203 **Discussion**

204 mRNA vaccine platforms responded rapidly to SARS-CoV-2 threat, demonstrating robust levels
205 of efficacy in adults(26, 27). However, despite the successes of SARS-CoV-2 vaccines, the global
206 roll out has begun to highlight key vulnerable populations, and strategic gaps, that may limit the
207 impact of vaccination globally. Although children generally experience mild symptoms, they can
208 harbor robust, high levels of SARS-CoV-2 replication, thereby contributing significantly to viral
209 spread(28-30). Furthermore, increasing numbers of children are suffering from severe COVID-19
210 with over 28,000 hospitalizations and over 700 deaths in the US alone as of December 2021 (31).
211 However, because children have a more naïve immune system that evolves with age it was
212 uncertain how the mRNA vaccine platforms would impact immunogenicity in young children.
213 Additionally, recent results suggest that dose adjustments for very young children, due to safety
214 and tolerance concerns, have introduced additional variation in immunogenicity, resulting in poor
215 immunogenicity in children under 5 years, who received a lower dose than the adult recommended
216 30µg dose (11). Thus, in the absence of empirical data, optimal dosing is uncertain. Thus, here we
217 aimed to dive deeply in defining humoral profile differences across doses and across children and
218 adults. Similar to results with the Pfizer and Moderna mRNA vaccine trials in teenagers (32, 33),
219 here we found that the Moderna mRNA vaccine was highly immunogenic in 6-11 year old
220 children, generating a humoral response superior to that seen following viral exposure. However,
221 granular vaccine-induced humoral profiling identified significant differences in adult and pediatric
222 vaccine responses, marked by a selective induction of highly functional IgG responses, with fewer
223 IgA and IgM responses compared to adults. At a matched 100µg dose, children mounted more

224 robust opsonophagocytic functions, and Fc γ -receptor binding compared to adults. Moreover, at
225 half the adult dose, children mounted equal, albeit more variable, responses compared to adults.

226 Virus neutralization represents a key surrogate marker of vaccine protection against COVID-19.
227 Yet despite the loss of neutralization against several emerging variants of concern (VOCs), mRNA
228 vaccines continue to provide protection against severe disease and death(21, 34). Interestingly,
229 opsonophagocytic functions of antibodies, rather than neutralization alone, have been linked to
230 survival of COVID-19 following natural infection(12) and are associated with protection from
231 infection in animal models(35, 36). Here, when immunized with the adult dose, children induced
232 comparable neutralization but exhibited a preferential expansion of opsonophagocytic functions
233 compared to adults. The enhanced opsonophagocytic function was not linked to differential
234 subclass or isotype selection, suggesting that children may induce more functional antibodies via
235 alternate changes to the humoral immune response, including potential differences in post-
236 translational IgG modification that may lead to more flexible, highly functional responses,
237 representing an evolutionary adaptation enabling children to react more flexibly to infections(37).

238 The adaptive immune response matures during the first decade of life(38). Several lines of
239 evidence suggest that the more naïve immune response in children may allow the immune system
240 to adapt and evolve more easily to new pathogens, poised to generate broader immunity to new
241 viruses(39, 40). Moreover, throughout life, our naïve clonal repertoire or immune cells shift in
242 response to the sequence of pathogens and vaccines we are exposed to. Thus, naïve children may
243 have a less “biased” repertoire, enabling the generation of immunity to a broader range of
244 pathogens(41). Along these lines, we observed robust induction of immunity against most VOCs,
245 with the exception of omicron. However, IgG and Fc-receptor binding profiles were highly similar
246 among children and adults, although 100 μ g immunized children induced IgG that were more

247 resilient against VOCs, exhibiting robust recognition of the omicron Spike, whereas both 50 μ g
248 immunized children and 100 μ g immunized adults both lost partial recognition of the omicron
249 Spike. These data suggest that higher pediatric dosing can result in more flexible humoral
250 immunity in children against highly divergent VOCs, superior to those induced in adults at a
251 matched dose. Thus, children may generate more functional Fc-effector functions, that while not
252 neutralizing, may be poised for rapid elimination of the pathogen upon transmission, providing a
253 highly effective means to prevent COVID-19.

254 With the increasing spread of SARS-CoV-2 omicron among younger populations (42), increasing
255 incidence of COVID-19 among the pediatric population, the rare incidence of MIS-C, and the
256 recent appreciation for long-COVID in children, the need to determine whether SARS-CoV-2
257 vaccines can elicit functional immune responses will be key to protect children(3, 5, 28, 43, 44).
258 Comparable to previous observations in adults(10), the mRNA-1273 vaccine induced robust
259 binding titers, neutralization, and Fc effector function in vaccinated children, in a dose dependent
260 manner, compared to children diagnosed with COVID-19 or MIS-C, pointing to the importance of
261 vaccination to robustly bolster immunity to SARS-CoV-2 and emerging VOCs to provide broader
262 and more potent immunity to SARS-CoV-2. Whether these responses will wane differentially
263 across doses, whether they will be more protective against particular VOCs, and whether children
264 will require boosting remains unclear, however, these findings support vaccination of children with
265 mRNA-1273 as a safe and effective strategy to protect children against COVID-19, MIS-C, and
266 Long-COVID.

267 **Contributions**

268 Y.C.B. and J.K. performed the serological experiments. K.J.D, E.C.L and A.B.B. performed the
269 neutralization assay. Y.C.B., L.M.Y. and G.A. analyzed and interpreted the data. M.D.B., E.J.F.,

270 J.P.D., B.P.B., A.G.F., A.F., W.S., D.Z., M.J., D.G., and L.M.Y. supervised and managed the
271 sample collection. G.A. supervised the project. Y.C.B., L.M.Y. and G.A. drafted the manuscript.
272 All authors critically reviewed the manuscript.

273

274 **Acknowledgment**

275 We thank Nancy Zimmerman, Mark and Lisa Schwartz, an anonymous donor (financial support),
276 Terry and Susan Ragon, and the SAMANA Kay MGH Research Scholars award for their support.
277 We acknowledge support from the Ragon Institute of MGH, MIT, and Harvard, the Massachusetts
278 Consortium on Pathogen Readiness (MassCPR), the NIH (3R37AI080289-11S1, R01AI146785,
279 U19AI42790-01, U19AI135995-02, U19AI42790-01, 1U01CA260476 – 01,
280 CIVIC75N93019C00052, 5K08HL143183), the Gates Foundation Global Health Vaccine
281 Accelerator Platform funding (OPP1146996 and INV-001650), and the Musk Foundation.

282 **Competing interests**

283 G.A. is a founder of Seromyx Systems, a company developing a platform technology that
284 describes the antibody immune response. G.A.'s interests were reviewed and are managed by
285 Massachusetts General Hospital and Partners HealthCare in accordance with their conflict of
286 interest policies. All other authors have declared that no conflicts of interest exist.

287

288

289 **Methods**

290 Cohort

291 Pediatric vaccinee samples were obtained from children who were vaccinated with two doses
292 100 µg mRNA-1273 at MGH as participants in Part 1 (open label) of a Phase2/3 clinical trial
293 (ClinicalTrials.gov Identifier: NCT04796896). Additionally, we included samples from eight
294 children who presented with acute PCR confirmed COVID-19 (7-19 years) or six children with
295 MIS-C (3-22 years) at our hospital. Additionally, samples from 14 adults who received two
296 doses mRNA-1273 as part of a phase 1 clinical trial were used as controls (ClinicalTrials.gov
297 Identifier: NCT04283461). All pediatric participants provided informed assent and their legal
298 guardian provided informed consent prior to participation in the MGH Pediatric COVID-19
299 Biorepository. Blood samples and symptom report via an IRB-approved symptom questionnaire
300 were collected prior to vaccination, one month after the first vaccination and one month after the
301 second vaccination. This study was overseen and approved by the MassGeneral Institutional
302 Review Board (IRB #2020P00955).

303 Antigens and biotinylation

304 All antigens were biotinylated using an NHS-Sulfo-LC-LC kit according to the manufacturer's
305 instruction (Thermo Fisher, MA, USA) if required by the assay and excessive biotin was removed
306 by size exclusion chromatography using Zeba-Spin desalting columns (7kDa cutoff, Thermo
307 Fisher).

308 Antibody isotype and Fc receptor binding

309 Antigen-specific antibody isotype and subclass titers and Fc receptor binding profiles were
310 analyzed with a custom multiplex Luminex assay as described previously (45). In brief, antigens

311 were coupled directly to Luminex microspheres (Luminex Corp, TX, USA). Coupled beads were
312 incubated with diluted plasma samples washed, and Ig isotypes or subclasses with a 1:100
313 diluted PE-conjugated secondary antibody for IgG1 (clone: HP6001), IgG2 (clone: 31-7-4), IgG3
314 (clone: HP6050), IgG4 (clone: HP6025), IgM (clone: SA-DA4), IgA1 (clone: B3506B4) or IgA2
315 (clone: A9604D2) (all Southern Biotech, AL, USA), respectively. For the Fc γ R binding, a
316 respective PE-streptavidin (Agilent Technologies) coupled recombinant and biotinylated human
317 Fc γ R protein was used as a secondary probe. Excessive secondary reagent was washed away
318 after 1h incubation, and the relative antigen-specific antibody levels were determined on an iQue
319 analyzer (Intellicyt).

320 Antibody-Dependent Complement Deposition (ADCD)

321 Complement deposition was performed as described before(46). In brief, biotinylated antigens
322 were coupled to FluoSphere NeutrAvidin beads (Thermo Fisher) and to form immune-complexes
323 incubated with 10 μ l 1:10 diluted plasma samples for 2h at 37°C. After non-specific antibodies
324 were washed away, immune-complexes were incubated with guinea pig complement in GVB++
325 buffer (Boston BioProducts, MA, USA) for 20 min at 37°C. EDTA containing PBS (15mM) was
326 used to stop the complement reaction and deposited C3 on beads was stained with anti-guinea pig
327 C3-FITC antibody (MP Biomedicals, CA, USA, 1:100, polyclonal) and analyzed on an iQue
328 analyzer (Intellicyt).

329 Antibody-Dependent-Neutrophil-Phagocytosis (ADNP)

330 Phagocytosis score of primary human neutrophils was determined as described before(47).
331 Biotinylated antigens were coupled to FluoSphere NeutrAvidin beads (Thermo Fisher) and
332 incubated with 10 μ l 1:100 diluted plasma for 2h at 37°C to form immune-complexes. Primary

333 neutrophils were derived from Ammonium-Chloride-Potassium (ACK) buffer lysed whole blood
334 from healthy donors and incubated with washed immune complexes for 1h at 37°C. Afterwards,
335 neutrophils were stained for surface CD66b (Biolegend, CA, USA; 1:100, clone: G10F5)
336 expression, fixed with 4% para-formaldehyde and analyzed on a iQue analyzer (Intellicyt).

337 Antibody-Dependent-THP-1 Cell-Phagocytosis (ADCP)

338 THP-1 phagocytosis assay was performed as described before(48). In brief, biotinylated antigens
339 were coupled to FluoSphere NeutrAvidin beads (Thermo Fisher) and incubated with 10 µl 1:100
340 diluted plasma for 2h at 37°C to form immune complexes. THP-1 monocytes were added to the
341 beads, incubated for 16 h at 37°C, fixed with 4% para-formaldehyde and analyzed on a iQue
342 analyzer (Intellicyt).

343 Antibody-Dependent-NK-Activation (ADNKA)

344 To determine Antibody-dependent NK cell activation, MaxiSporp ELISA plates (Thermo Fisher)
345 were coated with respective antigen for 2h at RT and then blocked with 5% BSA (Sigma-Aldrich).
346 50 µl 1:50 diluted plasma sample or monoclonal Abs was added to the wells and incubated
347 overnight at 4°C. NK cells were isolated from buffy coats from healthy donors using the
348 RosetteSep NK cell enrichment kit (STEMCELL Technologies, MA, USA) and stimulated with
349 rhIL-15 (1ng/ml, STEMCELL Technologies) at 37°C overnight. NK cells were added to the
350 washed ELISA plate and incubated together with anti-human CD107a (BD, 1:40, clone: H4A3),
351 brefeldin A (Sigma-Aldrich, MO, USA), and monensin (BD) for 5 hours at 37°C. Next, cells were
352 surface stained for CD56 (BD, 1:200, clone: B159), CD16 (BD, 1:200, clone: 3G8), and CD3 (BD,
353 1:800, UCHT1). After fixation and permeabilization with FIX & PERM Cell Permeabilization Kit
354 (Thermo Fisher), cells were stained for intracellular markers MIP1β (BD, 1:50, clone: D21-1351)

355 and IFN γ (BD, 1:17, clone: B27). NK cells were defined as CD3-CD16+CD56+ and frequencies
356 of degranulated (CD107a+), INF γ + and MIP1 β + NK cells determined on an iQue analyzer
357 (Intellicyt)(49).

358 Virus neutralization

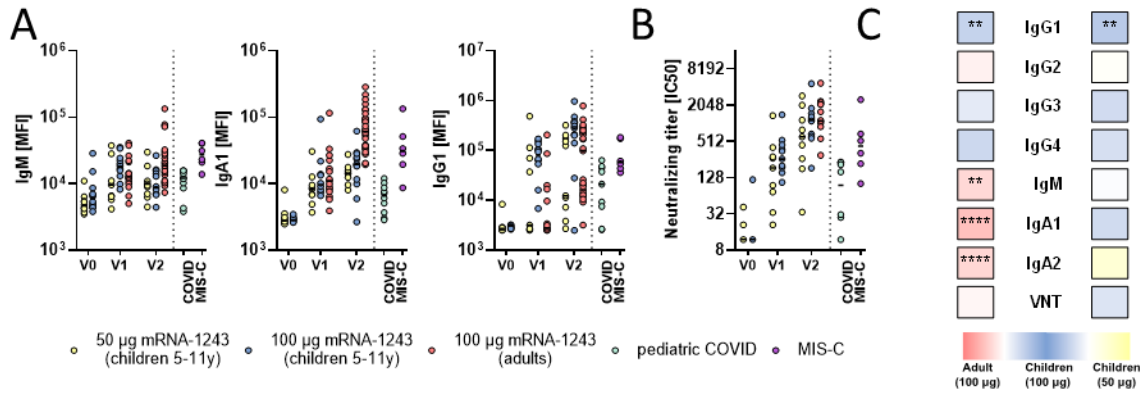
359 Three-fold serial dilutions ranging from 1:12 to 1:8748 were performed for each plasma sample
360 before adding 50–250 infectious units of pseudovirus expressing the SARS-CoV-2 reference
361 (Wuhan/wildtype) or delta variant Spike to hACE-2 expressing HEK293 cells for 1 hour.
362 Percentage neutralization was determined by subtracting background luminescence measured in
363 cell control wells (cells only) from sample wells and dividing by virus control wells (virus and
364 cells only). Pseudovirus neutralization titers (pNT50) values were calculated by taking the inverse
365 of the 50% inhibitory concentration value for all samples with a pseudovirus neutralization value
366 of 80% or higher at the highest concentration of serum.

367 Data analysis and Statistics

368 Data analysis was performed using GraphPad Prism (v.9.2.0) and RStudio (v.1.3 and R v.4.0).
369 Comparisons between the adults and children were performed using Wilcoxon-signed rank test
370 followed by Benjamini-Hochberg (BH) correction. Multivariate classification models were built
371 to discriminate humoral profiles between vaccination arms. Prior to analysis, all data were
372 normalized using z-scoring. Feature selection was performed using least absolute shrinkage and
373 selection operator (LASSO). Classification and visualization were performed using partial least
374 square discriminant analysis (PLS-DA). Model accuracy was assessed using ten-fold cross-
375 validation. These analyses were performed using R package “ropls” version 1.20.0 (50) and
376 “glmnet” version 4.0.2(51). Co-correlates of LASSO selected features were calculated to find

377 features that can equally contribute to discriminating vaccination arms. Correlations were
378 performed using Spearman method followed by Benjamini-Hochberg correction. The co-correlate
379 network was generated using R package “network” version 1.16.0(52).

380

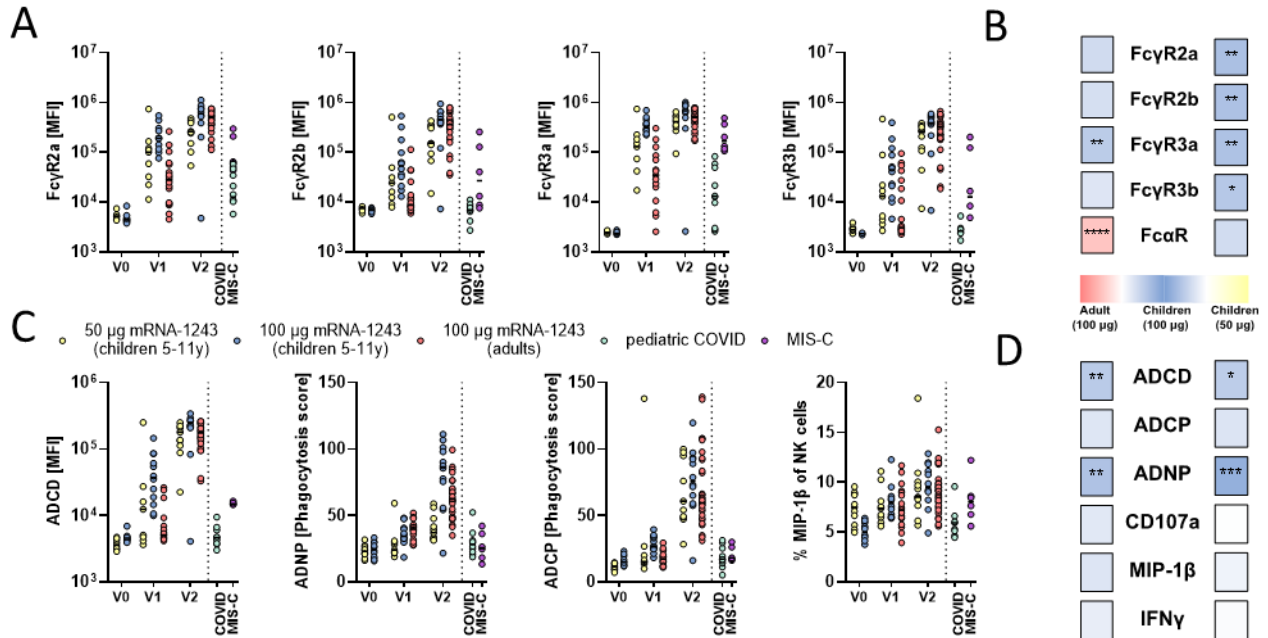


381

382 **Figure 1. mRNA-1273 vaccination induces robust binding and neutralizing titers in children**

383 A) Relative SARS-CoV-2 spike (Wuhan) specific IgM, IgA1 and IgG1 binding levels were
 384 determined by Luminex in children (6-11 years) receiving 50µg or 100µg mRNA1273 before
 385 (V0₅₀: n=12; V0₁₀₀: n=12), after the first (V1₅₀: n=9; V1₁₀₀: n=12) or after the second (V1₅₀: n=11;
 386 V2₁₀₀: n=12) dose or in adults receiving two 100µg doses (V1: n=19; V2: n=33) as well as in
 387 convalescent pediatric COVID (n=9) or MIS-C (n=6). B) The dot plots show the inverse 50 %
 388 virus neutralizing titers in children (6-11 years) receiving 50µg or 100µg mRNA1273 before (V0₅₀:
 389 n=12; V0₁₀₀: n=12), after the first (V1₅₀: n=9; V1₁₀₀: n=12) or after the second (V1₅₀: n=9; V2₁₀₀:
 390 n=11) dose or in adults receiving two 100µg doses (V2: n=14) as well as in convalescent pediatric
 391 COVID (n=9) or MIS-C (n=6). C) Heatmap strips summarize univariate comparison at the V2
 392 timepoint of 100µg dose vaccinated children to adults (left panel) or to 50µg dose vaccinated
 393 children (right panel). Color of the tiles indicate whether antibody binding titer were upregulated
 394 in the respective group: 100µg vaccinated children (blue shades), adults (red shades), or 50µg
 395 vaccinated children (yellow shades). A Wilcoxon-rank test was used to test for statistical
 396 significance and asterisks indicate statistically significant differences of the respective feature after
 397 Benjamini-Hochberg correction for multiple testing (*:p<0.05; **:p<0.01;***:p<0.001).

398



399

400 **Figure 2. mRNA-1273 vaccination induces higher FcγR binding and phagocytic activity in**

401 **children.** A) Binding of SARS-CoV-2 specific antibodies to FcγR2a, 2b, 3a, and 3b was

402 determined by Luminex in children (6-11 years) receiving 50µg or 100µg mRNA1273 before

403 (V0₅₀: n=12; V0₁₀₀: n=12), after the first (V1₅₀: n=9; V1₁₀₀: n=12) or after the second (V1₅₀: n=11;

404 V2₁₀₀: n=12) dose or in adults receiving two 100µg doses (V1: n=19; V2: n=33) as well as in

405 convalescent pediatric COVID (n=9) or MIS-C (n=6). C) Heatmap strips summarize univariate

406 comparison of Fc receptor binding at the V2 timepoint of 100µg dose vaccinated children to adults

407 (left panel) or to 50µg dose vaccinated children (right panel). Color of the tiles indicate whether

408 antibody binding titer were upregulated in the respective group: 100µg vaccinated children (blue

409 shades), adults (red shades), or 50µg vaccinated children (yellow shades). C) The ability of SARS-

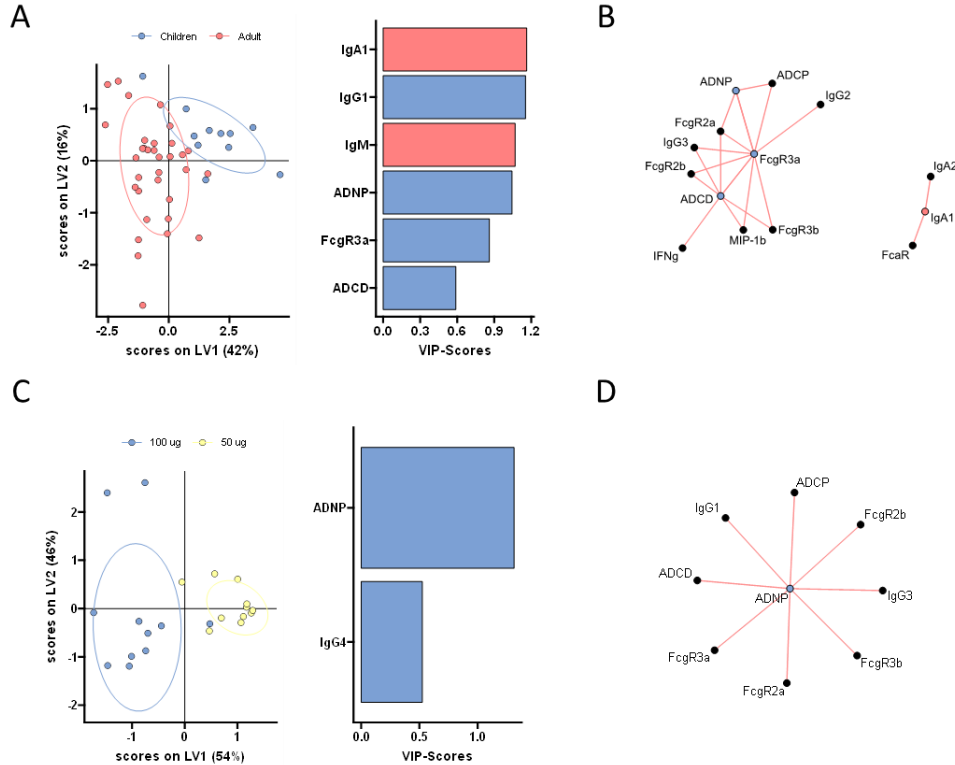
410 CoV-2 S specific antibody Fc to induce antibody-dependent-complement-deposition (ADCC),

411 neutrophil-phagocytosis (ADNP), cellular-THP1 monocyte-phagocytosis (ADCP), or activation

412 of NK cells marked by expression of MIP-1β was analyzed. D) Heatmap strips summarize

413 univariate comparison of Fc effector functions at the V2 timepoint of 100 μ g dose vaccinated
414 children to adults (left panel) or to 50 μ g dose vaccinated children (right panel) as in B). A
415 Wilcoxon-rank test was used to test for statistical significance in C) and D) and asterisks indicate
416 statistically significant differences of the respective feature after Benjamini-Hochberg correction
417 for multiple testing (*:p<0.05; **:p<0.01;***:p<0.001).

418



419

420

421 **Figure 3. Distinct humoral profiles distinguish between adult and pediatric vaccine**

422 **responses.** A) A machine learning model was built using a minimal set of LASSO selected SARS-

423 CoV-2 S specific features at V2 (left panel) to discriminate between vaccine responses in adult

424 (red) and 100 μ g vaccinated children (purple) in a PLS-DA analysis (right panel). B) The co-

425 correlation network illustrates all LASSO-selected features. Nodes of selected features are colored

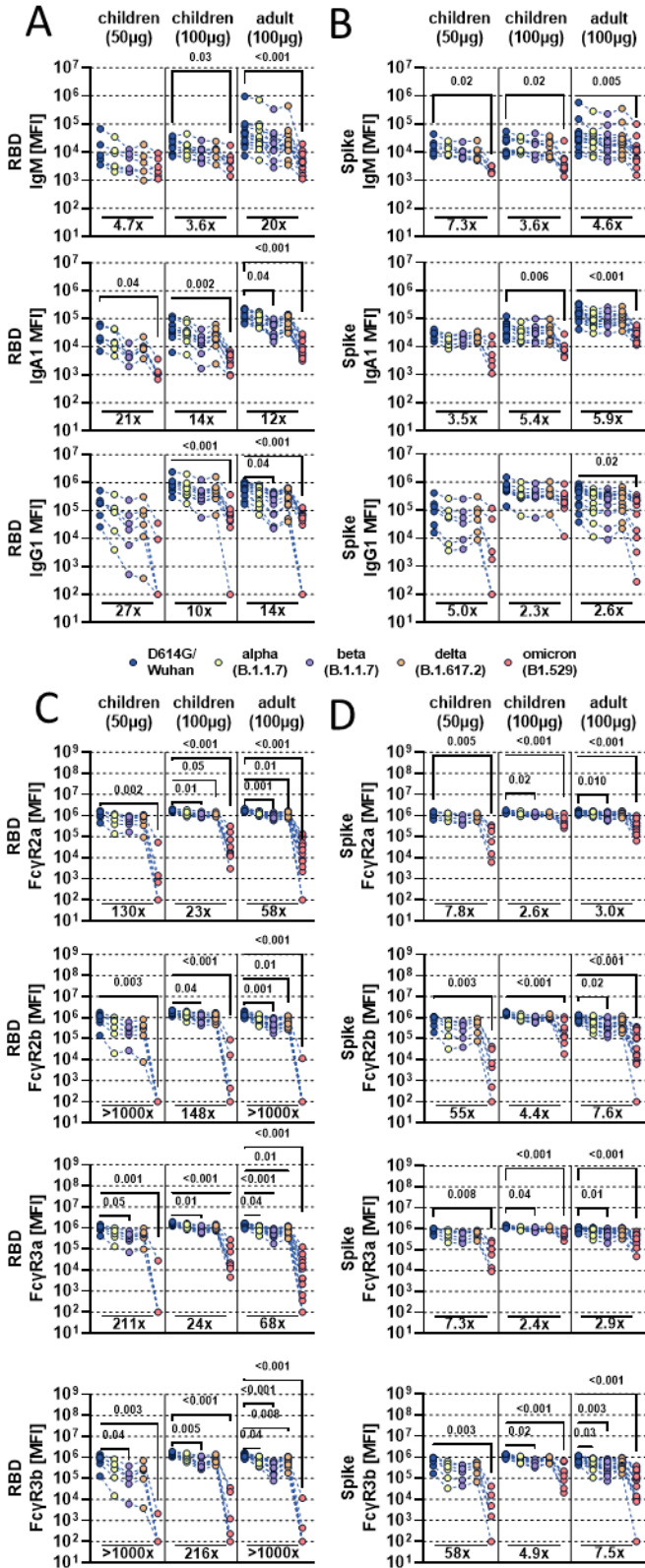
426 whether they were enriched in children (purple) or adults (red). Lines indicate significant ($p < 0.05$)

427 spearman correlations with $|r| > 0.7$ of connected features (only positive correlations with $r > 0$ were

428 observed). C) PLS-DA model of LASSO selected features at V2 (left panel) to discriminate

429 between vaccine responses in 100 μ g (purple) and 50 μ g (yellow) vaccinated children. D) The co-

430 correlation network as in B) illustrates all LASSO-selected features. Nodes of selected features are
431 colored whether they were enriched in 100 μ g vaccinated children (purple).



433 **Figure 4. mRNA-1273 vaccination elicits humoral responses to SARS-CoV-2 variants of**
434 **concern.** A-B) The line graphs show the vaccine induced IgM, IgA1 and IgG1 recognition to
435 D614G (WT; blue), alpha (B.1.117; yellow), beta (B.1.351; purple), delta (B.1.617.2; orange), and
436 omicron (B.1.529; red) variants of concern receptor binding domains (A) or full Spike (B) for
437 children ($n_{50\mu\text{g}}=6$, $n_{100\mu\text{g}}=9$) or adults ($n=14$) at V2, where each individuals' response is linked
438 across VOC antigens. C-D) The line graphs show the Fc γ R (Fc γ R2a, Fc γ R2b, Fc γ R3a, Fc γ R3b)
439 binding profiles of vaccine induced antibodies to RBD or Spike VOC antigens across children
440 ($n_{50\mu\text{g}}=6$, $n_{100\mu\text{g}}=9$) or adults ($n=12$) at V2, where each individuals' response is linked across VOC
441 antigens. Background corrected data is shown and negative values were set to 100 for graphing
442 purposes in A-D. A Kruskal-Wallis test with a Benjamini-Hochberg post-test correction for
443 multiple comparisons was used to test for statistical differences between wildtype and VOC titers
444 within groups. P-values for significantly different features are shown above and fold change
445 reduction of omicron titer compared to wildtype below each dataset.

446

447

448

449

450

451

452

453

454 **Reference**

- 455 1. G. Matias *et al.*, Estimates of hospitalization attributable to influenza and RSV in the US
456 during 1997-2009, by age and risk status. *BMC Public Health* **17**, 271 (2017).
- 457 2. J. F. Ludvigsson, Systematic review of COVID-19 in children shows milder cases and a
458 better prognosis than adults. *Acta Paediatr* **109**, 1088-1095 (2020).
- 459 3. D. A. Siegel *et al.*, Trends in COVID-19 Cases, Emergency Department Visits, and
460 Hospital Admissions Among Children and Adolescents Aged 0-17 Years - United States,
461 August 2020-August 2021. *MMWR Morb Mortal Wkly Rep* **70**, 1249-1254 (2021).
- 462 4. CDC.gov, CenterForDiseaseControlAndPrevention.
- 463 5. M. J. Delahoy *et al.*, Hospitalizations Associated with COVID-19 Among Children and
464 Adolescents - COVID-NET, 14 States, March 1, 2020-August 14, 2021. *MMWR Morb*
465 *Mortal Wkly Rep* **70**, 1255-1260 (2021).
- 466 6. L. R. Feldstein *et al.*, Multisystem Inflammatory Syndrome in U.S. Children and
467 Adolescents. *N Engl J Med* **383**, 334-346 (2020).
- 468 7. E. J. Schatorje, G. J. Driessen, R. W. van Hout, M. van der Burg, E. de Vries, Levels of
469 somatic hypermutations in B cell receptors increase during childhood. *Clin Exp Immunol*
470 **178**, 394-398 (2014).
- 471 8. Z. A. Bhutta, R. E. Black, Global maternal, newborn, and child health--so near and yet so
472 far. *N Engl J Med* **369**, 2226-2235 (2013).
- 473 9. J. Bonhoeffer, C. A. Siegrist, P. T. Heath, Immunisation of premature infants. *Arch Dis*
474 *Child* **91**, 929-935 (2006).
- 475 10. L. A. Jackson *et al.*, An mRNA Vaccine against SARS-CoV-2 - Preliminary Report. *N*
476 *Engl J Med* **383**, 1920-1931 (2020).

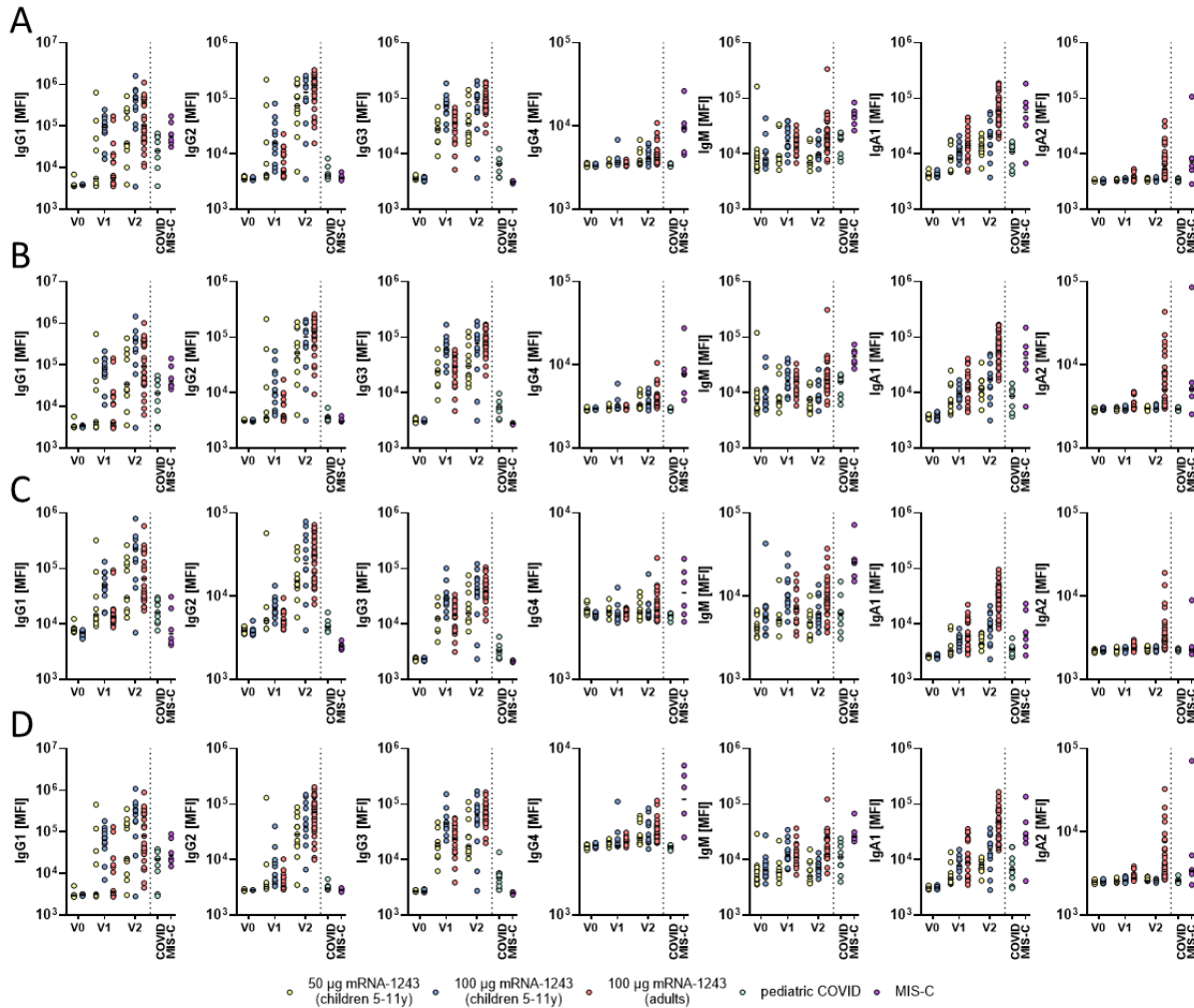
- 477 11. Press Release Pfizer Inc and BioNTech SE PFIZER AND BIONTECH PROVIDE
478 UPDATE ON ONGOING STUDIES OF COVID-19 VACCINE. (2021).
- 479 12. T. Zohar *et al.*, Compromised Humoral Functional Evolution Tracks with SARS-CoV-2
480 Mortality. *Cell* **183**, 1508-1519 e1512 (2020).
- 481 13. C. E. Z. Chan *et al.*, The Fc-mediated effector functions of a potent SARS-CoV-2
482 neutralizing antibody, SC31, isolated from an early convalescent COVID-19 patient, are
483 essential for the optimal therapeutic efficacy of the antibody. *PLoS One* **16**, e0253487
484 (2021).
- 485 14. M. J. Gorman *et al.*, Fab and Fc contribute to maximal protection against SARS-CoV-2
486 following NVX-CoV2373 subunit vaccine with Matrix-M vaccination. *Cell Rep Med*,
487 100405 (2021).
- 488 15. T. Andrews, K. E. Sullivan, Infections in patients with inherited defects in phagocytic
489 function. *Clin Microbiol Rev* **16**, 597-621 (2003).
- 490 16. D. N. Forthal, C. Moog, Fc receptor-mediated antiviral antibodies. *Curr Opin HIV AIDS*
491 **4**, 388-393 (2009).
- 492 17. S. Chakraborty *et al.*, Proinflammatory IgG Fc structures in patients with severe COVID-
493 19. *Nat Immunol* **22**, 67-73 (2021).
- 494 18. E. R. Stiehm, H. H. Fudenberg, Serum levels of immune globulins in health and disease: a
495 survey. *Pediatrics* **37**, 715-727 (1966).
- 496 19. J. M. Woof, M. A. Kerr, IgA function--variations on a theme. *Immunology* **113**, 175-177
497 (2004).
- 498 20. E. J. Haas *et al.*, Impact and effectiveness of mRNA BNT162b2 vaccine against SARS-
499 CoV-2 infections and COVID-19 cases, hospitalisations, and deaths following a

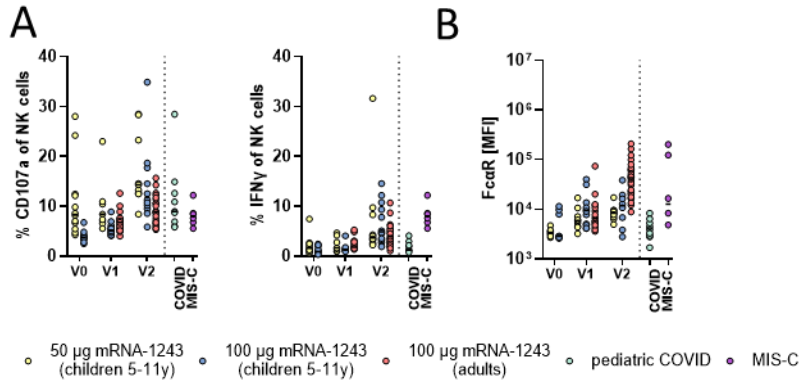
- 500 nationwide vaccination campaign in Israel: an observational study using national
501 surveillance data. *Lancet* **397**, 1819-1829 (2021).
- 502 21. J. S. Tregoning, K. E. Flight, S. L. Higham, Z. Wang, B. F. Pierce, Progress of the COVID-
503 19 vaccine effort: viruses, vaccines and variants versus efficacy, effectiveness and escape.
504 *Nat Rev Immunol* **21**, 626-636 (2021).
- 505 22. L. J. Abu-Raddad, H. Chemaitelly, A. A. Butt, C.-V. National Study Group for,
506 Effectiveness of the BNT162b2 Covid-19 Vaccine against the B.1.1.7 and B.1.351
507 Variants. *N Engl J Med* **385**, 187-189 (2021).
- 508 23. L. A. VanBlargan *et al.*, An infectious SARS-CoV-2 B.1.1.529 Omicron virus escapes
509 neutralization by several therapeutic monoclonal antibodies. *bioRxiv*,
510 2021.2012.2015.472828 (2021).
- 511 24. D. Planas *et al.*, Considerable escape of SARS-CoV-2 variant Omicron to antibody
512 neutralization. *bioRxiv*, 2021.2012.2014.472630 (2021).
- 513 25. P. Kaplonek *et al.*, Subtle immunological differences in mRNA-1273 and BNT162b2
514 COVID-19 vaccine induced Fc-functional profiles. *bioRxiv*, (2021).
- 515 26. L. R. Baden *et al.*, Efficacy and Safety of the mRNA-1273 SARS-CoV-2 Vaccine. *N Engl*
516 *J Med* **384**, 403-416 (2021).
- 517 27. F. P. Polack *et al.*, Safety and Efficacy of the BNT162b2 mRNA Covid-19 Vaccine. *N*
518 *Engl J Med* **383**, 2603-2615 (2020).
- 519 28. V. T. Chu *et al.*, Household Transmission of SARS-CoV-2 from Children and Adolescents.
520 *N Engl J Med* **385**, 954-956 (2021).

- 521 29. L. M. Yonker *et al.*, Pediatric Severe Acute Respiratory Syndrome Coronavirus 2 (SARS-
522 CoV-2): Clinical Presentation, Infectivity, and Immune Responses. *J Pediatr* **227**, 45-52
523 e45 (2020).
- 524 30. L. M. Yonker *et al.*, Virologic features of SARS-CoV-2 infection in children. *J Infect Dis*,
525 (2021).
- 526 31. C. B., H. M., "Children and COVID-19: State Data Report A joint report from the
527 American Academy of Pediatrics and the Children's Hospital Association," (American
528 Academy of Pediatrics and Children's Hospital Association,
529 [https://downloads.aap.org/AAP/PDF/AAP%20and%20CHA%20-
530 %20Children%20and%20COVID-
531 19%20State%20Data%20Report%2012.23%20FINAL.pdf](https://downloads.aap.org/AAP/PDF/AAP%20and%20CHA%20-%20Children%20and%20COVID-19%20State%20Data%20Report%2012.23%20FINAL.pdf), 2021).
- 532 32. R. W. Frenck, Jr. *et al.*, Safety, Immunogenicity, and Efficacy of the BNT162b2 Covid-19
533 Vaccine in Adolescents. *N Engl J Med* **385**, 239-250 (2021).
- 534 33. K. Ali *et al.*, Evaluation of mRNA-1273 SARS-CoV-2 Vaccine in Adolescents. *N Engl J*
535 *Med*, (2021).
- 536 34. K. Wu *et al.*, Serum Neutralizing Activity Elicited by mRNA-1273 Vaccine. *N Engl J Med*
537 **384**, 1468-1470 (2021).
- 538 35. K. McMahan *et al.*, Correlates of protection against SARS-CoV-2 in rhesus macaques.
539 *Nature* **590**, 630-634 (2021).
- 540 36. J. R. Francica *et al.*, Protective antibodies elicited by SARS-CoV-2 spike protein
541 vaccination are boosted in the lung after challenge in nonhuman primates. *Sci Transl Med*
542 **13**, (2021).

- 543 37. G. Alter, T. H. M. Ottenhoff, S. A. Joosten, Antibody glycosylation in inflammation,
544 disease and vaccination. *Semin Immunol* **39**, 102-110 (2018).
- 545 38. A. K. Simon, G. A. Hollander, A. McMichael, Evolution of the immune system in humans
546 from infancy to old age. *Proc Biol Sci* **282**, 20143085 (2015).
- 547 39. A. Vatti *et al.*, Original antigenic sin: A comprehensive review. *J Autoimmun* **83**, 12-21
548 (2017).
- 549 40. J. J. Goronzy, C. M. Weyand, T cell development and receptor diversity during aging. *Curr*
550 *Opin Immunol* **17**, 468-475 (2005).
- 551 41. L. Garderet *et al.*, The umbilical cord blood alphabeta T-cell repertoire: characteristics of
552 a polyclonal and naive but completely formed repertoire. *Blood* **91**, 340-346 (1998).
- 553 42. P. Elliott *et al.*, Rapid increase in Omicron infections in England during December 2021:
554 REACT-1 study. *medRxiv*, 2021.2012.2022.21268252 (2021).
- 555 43. I. M. Osmanov *et al.*, Risk factors for long covid in previously hospitalised children using
556 the ISARIC Global follow-up protocol: A prospective cohort study. *Eur Respir J*, (2021).
- 557 44. A. B. Payne *et al.*, Incidence of Multisystem Inflammatory Syndrome in Children Among
558 US Persons Infected With SARS-CoV-2. *JAMA Netw Open* **4**, e2116420 (2021).
- 559 45. E. P. Brown *et al.*, High-throughput, multiplexed IgG subclassing of antigen-specific
560 antibodies from clinical samples. *J Immunol Methods* **386**, 117-123 (2012).
- 561 46. S. Fischinger *et al.*, A high-throughput, bead-based, antigen-specific assay to assess the
562 ability of antibodies to induce complement activation. *J Immunol Methods* **473**, 112630
563 (2019).
- 564 47. C. B. Karsten *et al.*, A versatile high-throughput assay to characterize antibody-mediated
565 neutrophil phagocytosis. *J Immunol Methods* **471**, 46-56 (2019).

- 566 48. M. E. Ackerman *et al.*, A robust, high-throughput assay to determine the phagocytic
567 activity of clinical antibody samples. *Journal of immunological methods* **366**, 8-19 (2011).
- 568 49. L. L. Lu *et al.*, A Functional Role for Antibodies in Tuberculosis. *Cell* **167**, 433-443 e414
569 (2016).
- 570 50. E. A. Thevenot, A. Roux, Y. Xu, E. Ezan, C. Junot, Analysis of the Human Adult Urinary
571 Metabolome Variations with Age, Body Mass Index, and Gender by Implementing a
572 Comprehensive Workflow for Univariate and OPLS Statistical Analyses. *J Proteome Res*
573 **14**, 3322-3335 (2015).
- 574 51. J. H. Friedman, T. Hastie, R. Tibshirani, Regularization Paths for Generalized Linear
575 Models via Coordinate Descent. *2010* **33**, 22 (2010).
- 576 52. C. T. Butts, network: a Package for Managing Relational Data in R. *Journal of Statistical*
577 *Software* **24**, (2008).





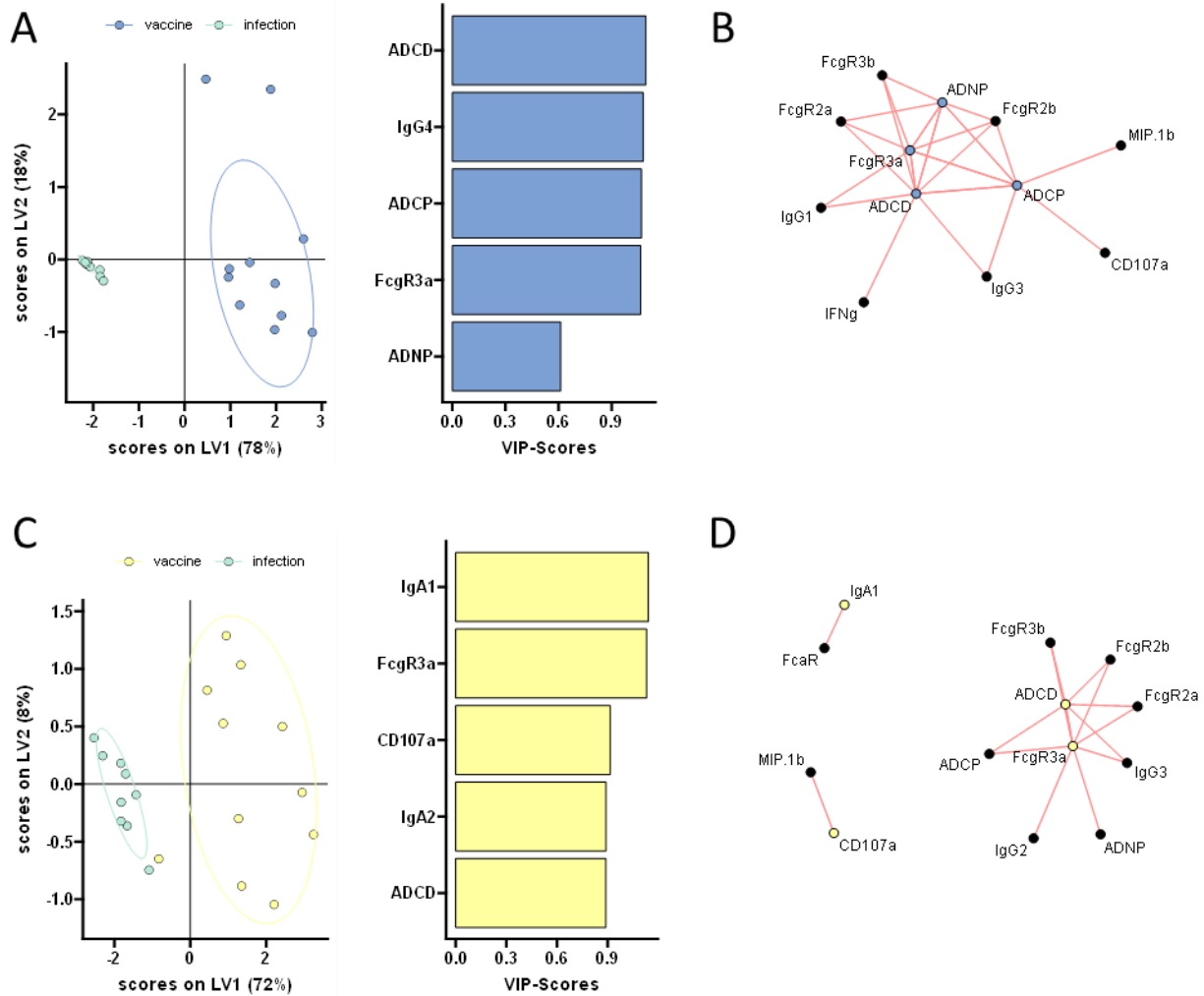
583

584 **Supplemental Figure 2. Univariate comparisons across vaccine profiles in children and**

585 **adults.** A) The plots show the antibody dependent NK cell activating (ADNKA, CD107a and IFN

586 γ expression) levels in children and adults to the SARS-CoV-2 wt spike. B) The plots show the

587 binding of SARS-CoV-2 wildtype specific IgA antibodies to Fc α R by Luminex.



588

589 **Supplemental Figure 3. Distinct humoral profiles in naturally infected and vaccinated**

590 **children.** A machine learning model was built to compare SARS-CoV-2 profiles in naturally

591 infected and 100 μg (A) or 50 μg (C) vaccinated children. A minimal set of LASSO selected

592 SARS-CoV-2 S specific features (left panel) were first selected and used to discriminate pediatric

593 vaccine responses (at V2) from natural infection (acute COVID) in children. Only five features

594 were sufficient to completely separate the two groups. A co-correlate network was used to define
595 additional features that differed in infection 100 μ g (B) or 50 μ g (D) vaccinated in children.

596